

# Living radical polymerization of styrene mediated by a piperidinyl-*N*-oxyl radical having very bulky substituents

Md. Abdul Mannan, Ayako Ichikawa, Yozo Miura\*

Department of Applied Chemistry, Graduate School of Engineering, Osaka City University, Sumiyoshi-ku, Osaka 558-8585, Japan

Received 29 September 2006; received in revised form 4 December 2006; accepted 5 December 2006

Available online 22 December 2006

## Abstract

A new cyclic nitroxide **1** and the corresponding alkoxyamines **9** and **10** were synthesized and the polymerization of styrene (St) initiated with **10** was investigated. The NO–C bond of **9** is very weak, cleaving at room temperature. On the other hand, alkoxyamine **10** is stable at room temperature and the  $A_{\text{act}}$  and  $E_{\text{act}}$  for the NO–C bond homolysis were determined to be  $1.4 \times 10^{15} \text{ s}^{-1}$  and  $124.5 \text{ kJ mol}^{-1}$ , respectively. When the polymerization of St was carried out at  $70^\circ\text{C}$ , the resultant poly(St) showed narrow polydispersities below 1.25. In the polymerization at  $90^\circ\text{C}$ , the resulting poly(St) showed narrow polydispersity until 60% conversion, but  $M_w/M_n$  was rapidly increased above 60% conversion. On the other hand, the polymerization at  $120^\circ\text{C}$  gave poly(St) with broad polydispersities. The unusual polymerization behavior was discussed on the basis of the SEC and ESR results.

© 2006 Elsevier Ltd. All rights reserved.

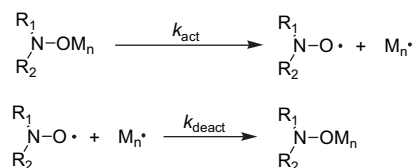
**Keywords:** Styrene; Living radical polymerization; Nitroxide

## 1. Introduction

Since the pioneering work by Rizzardo et al. [1] and Georges et al. [2], living radical polymerization (LRP) has attracted much attention not only as a convenient method to realize controlled molecular weights and narrow polydispersities but also as an excellent method for the syntheses of a variety of well-defined polymeric architectures. Nitroxide-mediated radical polymerization (NMRP) is one of the most useful methods for LRP [3,4], as well as atom transfer radical polymerization [5,6] and reversible addition–fragmentation chain transfer [7]. For the last decade, numerous nitroxides have been investigated to evaluate the abilities to control the radical polymerization and the mechanism for NMRP has widely been investigated [8–10]. Such great effort has greatly extended applicable monomers in NMRP [4,11–13].

In the NMRP process the reversible deactivation of the growing chain by persistent nitroxide is established. The

most important factors to determine the abilities of nitroxides to control the radical polymerization are the magnitudes of  $k_{\text{act}}$ ,  $k_{\text{deact}}$ , and  $K (=k_{\text{act}}/k_{\text{deact}})$  (Scheme 1), where  $k_{\text{act}}$  and  $k_{\text{deact}}$  mean the rate constants for the reversible activation of dormant species and the reversible deactivation of propagating chain by the coupling reaction of propagating chain and nitroxide, respectively. If both  $k_{\text{act}}$  and  $k_{\text{deact}}$  are large enough relative to the rate constant of propagation  $k_p$  and the concentrations of propagating chains are sufficiently low (i.e.,  $K$  is in the proper range), the polymerization systems proceed in the living fashion. However, if  $K$  is too large, that is, exceeds a critical value, the livingness will break down.

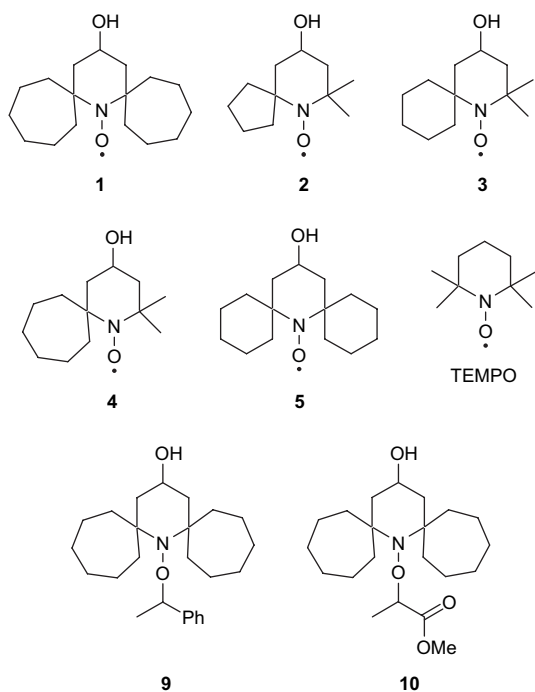


Scheme 1.

\* Corresponding author. Tel.: +81 6 6605 2798; fax: +81 6 6605 2769.

E-mail address: miura@a-chem.eng.osaka-cu.ac.jp (Y. Miura).

The rate constant  $k_{act}$  depends on the bond dissociation energy of the NO–C bond of the dormant species. Provided that leaving alkyl radicals are the same, the bond dissociation energy depends on the steric crowding around the N–O moiety and polar effects of nitroxide [14,15]. We previously investigated the polymerization of styrene (St) in the presence of **2–5** and TEMPO at 80–120 °C and showed that the abilities to control the polymerization of St were in the order: **5**  $\approx$  **4** > **3** > **2**  $\approx$  TEMPO [16–19]. This order clearly indicates that they are parallel to the steric crowding around the N–O moiety of the nitroxides. In this report we describe the syntheses of nitroxide **1** and the corresponding alkoxyamines **9** and **10** and the bulk polymerization of St at 70–120 °C in the presence of **1**.



## 2. Experimental section

### 2.1. General

IR spectra were run on a JASCO FT/IR-230 spectrophotometer.  $^1\text{H}$  NMR spectra were recorded with a JEOL  $\alpha$ -400 spectrometer. Chemical shifts ( $\delta$ ) are expressed in ppm downfield from tetramethylsilane as internal standard. High-resolution FAB mass spectra (HRFABMS) were measured on a JEOL JMS-AX500 spectrometer. Preparative HPLC (high-performance liquid chromatography) purification was carried out with a Japan Analytical Industry LC-908 recycling preparative HPLC instrument with  $\text{CHCl}_3$  as the eluant. Size exclusion chromatography (SEC) was performed with a Tosoh 8020 series using TSKgel G5000H<sub>HR</sub>, MultiporeH<sub>XL</sub>-M, and GMH<sub>HR</sub>-L columns calibrated with polystyrene standards, eluting with THF at 40 °C. Detection was made with a Tosoh refractive index detector RI8020.

### 2.2. Materials

2,2,4,6,6-Pentamethyl-1,2,5,6-tetrahydropyrimidine (acetoin) monohydrate was prepared by the reaction of acetone with ammonia in the presence of  $\text{NH}_4\text{SCN}$  according to the reported method [20]. Di-*tert*-butyl diperoxyoxalate was obtained according to the reported method [21]. Styrene (St) was purified by distillation under reduced pressure prior to use. Column chromatography was carried out on silica gel (Kanto Chemical N60 silica gel) or alumina (Merck aluminium oxide 90).

### 2.3. 8-Aza-17-hydroxydispiro[6.1.6.3]octadecane-8-yloxy (**1**)

#### 2.3.1. 8-Aza-17-oxodispiro[6.1.6.3]octadecane (**6**)

A mixture of acetoin monohydrate (30 g, 0.174 mol), cycloheptanone (95 g, 0.85 mol) and  $\text{NH}_4\text{Cl}$  (9.0 g) was heated at 60 °C for 10 h with stirring under nitrogen. After the mixture was cooled to room temperature, 10% HCl (350 mL) was added and the unreacted cycloheptanone was removed by extraction with ether. NaOH (50%, 350 mL) was then added to the aqueous layer and the organic layer was extracted with ether. The combined ether extracts were washed with brine, dried over anhydrous  $\text{MgSO}_4$ , and evaporated under reduced pressure. The residue was then chromatographed on silica gel with 1:5 ethyl acetate (EtOAc)–hexane to give **6** in 1.9% yield (0.87 g, 3.3 mmol). Crystallization from hexane gave colorless needles with mp 101–103 °C. IR (KBr): 3300 (NH), 1700  $\text{cm}^{-1}$  (C=O).  $^1\text{H}$  NMR ( $\text{CDCl}_3$ ):  $\delta$  1.30–1.70 (m, spirocycloheptyl, 24H), 2.23 (s,  $\text{CH}_2\text{COCH}_2$ , 4H). Calcd for  $\text{C}_{17}\text{H}_{29}\text{NO}$ : C 77.51, H 11.10, N 5.32. Found: C 77.39, H 11.23, N 5.24.

#### 2.3.2. 8-Aza-17-hydroxydispiro[6.1.6.3]octadecane (**7**)

$\text{NaBH}_4$  (1.68 g, 44.8 mmol) was added to a stirred solution of **6** (2.00 g, 7.6 mmol) in ethanol (EtOH) (50 mL) at room temperature. After the complete disappearance of **6** was confirmed by thin layer chromatography (TLC), water (200 mL) was added, and the resultant mixture was extracted with EtOAc. The combined EtOAc extracts were washed with brine, dried over anhydrous  $\text{MgSO}_4$ , and evaporated under reduced pressure. The residue was then chromatographed on silica gel with 1:2 EtOAc–hexane to give **7** in 88% yield (1.78 g, 6.7 mmol). Crystallization from hexane gave colorless needles with mp 107–109 °C. IR (KBr): 3400 (OH), 3300  $\text{cm}^{-1}$  (NH).  $^1\text{H}$  NMR ( $\text{CDCl}_3$ ):  $\delta$  0.89 (dd, each  $J = 12$  Hz,  $\text{CHHCH}(\text{OH})\text{CHH}$ , 2H), 1.70–1.98 (m, spirocycloheptyl, 24H), 1.96 (dd,  $J = 12$  and 4.1 Hz,  $\text{CHHCH}(\text{OH})\text{CHH}$ , 2H), 3.95 (tt,  $J = 4.1$  and 12 Hz,  $\text{CH}_2\text{CH}(\text{OH})\text{CH}_2$ , 1H). Calcd for  $\text{C}_{17}\text{H}_{31}\text{NO}$ : C 76.92, H 11.77, N 5.28. Found: C 76.76, H 11.92, N 5.08.

#### 2.3.3. 8-Aza-17-hydroxydispiro[6.1.6.3]octadecane-8-yloxy (**1**)

A mixture of **7** (1.0 g, 3.8 mmol), 35%  $\text{H}_2\text{O}_2$  (1.2 mL), Triton B (0.75 mL), and  $\text{Na}_2\text{WO}_4 \cdot 2\text{H}_2\text{O}$  (0.40 g) in methanol (MeOH) (15 mL) was stirred at room temperature for three days.  $\text{K}_2\text{CO}_3$  (10%, 10 mL) was then added to basify the

reaction mixture, and the resultant mixture was extracted three times with EtOAc. The combined EtOAc extracts were washed with brine, dried over anhydrous  $\text{MgSO}_4$ , and evaporated under reduced pressure. The residue was then chromatographed on alumina with 1:1 EtOAc–hexane to give **1** in 96% yield (1.04 g, 3.7 mmol). Recrystallization from hexane gave light red needles with mp 165–168 °C. IR (KBr):  $3400\text{ cm}^{-1}$  (OH). ESR (benzene):  $a_N = 1.533\text{ mT}$ ,  $g = 2.0060$ . Calcd for  $\text{C}_{17}\text{H}_{30}\text{NO}_2$ : C 72.81, H 10.78, N 4.99. Found: C 72.75, H 10.85, N 4.96.

#### 2.4. *N*-(1-Phenylethoxy)-8-aza-17-hydroxydispiro[6.1.6.3]octadecane (**9**)

A solution of **1** (0.34 g, 1.2 mmol) and di-*tert*-butyl diperoxyoxalate (DBDPX) (0.42 g, 1.8 mmol) in ethylbenzene (15 mL) was stirred at 35 °C for 5 h under a nitrogen stream. Concentration of the mixture to 2–3 mL and subsequent column chromatography on silica gel with 1:2 EtOAc–hexane gave **9** as a viscous oil, which contained some amounts of impurities. Although the oil was purified with a preparative recycling HPLC instrument, the complete purification was impossible due to the homolysis of the weak NO–C bond during the purification process.

#### 2.5. *N*-[1-(Methoxycarbonyl)ethoxy]-8-aza-17-hydroxydispiro[6.1.6.3]octadecane (**10**)

Nitroxide **1** (388 mg, 1.38 mmol), methyl 2-bromopropionate (193 mg, 1.15 mmol), powdery Cu (77 mg),  $\text{Cu(II)(OTf)}_2$  (OTf: trifluoromethanesulfonate) (4.1 mg,  $1.15 \times 10^{-2}$  mmol), 4,4'-di-*tert*-butyl-2,2'-dipyridyl (dTdp) (12.3 mg,  $4.62 \times 10^{-2}$  mmol), and benzene (5.0 mL) were put in a Pyrex glass tube, the mixture was degassed by three freeze–pump–thaw cycles with a high vacuum system, and the tube was sealed off. After being heated at 75 °C for 4 h, the mixture was evaporated under reduced pressure, and the residue was chromatographed on alumina with 1:1 hexane–EtOAc to remove the powdery Cu,  $\text{Cu(II)(OTf)}_2$ , and 4,4'-di-*tert*-butyl-2,2'-dipyridyl. The resulting oil was then purified with a preparative recycling HPLC with  $\text{CHCl}_3$  as the eluant. Yield 48% (0.20 mg, 0.55 mmol). HRFABMS:  $m/z$  Calcd for  $\text{C}_{21}\text{H}_{38}\text{NO}_4$  ( $\text{M} + \text{H}$ )<sup>+</sup> 368.2801. Found 368.2791.  $^1\text{H NMR}$  ( $\text{CDCl}_3$ ):  $\delta$  0.89 (dd, each  $J = 12\text{ Hz}$ ,  $\text{CHHCH(OH)CHH}$ , 2H), 1.70–1.98 (m, spiro-cycloheptyl, 24H), 1.96 (dd,  $J = 12$  and  $4.1\text{ Hz}$ ,  $\text{CHHCH(OH)CHH}$ , 2H), 1.46 (d,  $J = 6.8\text{ Hz}$ ,  $\text{C(=O)CH(CH}_3\text{)O}$ , 3H), 3.95 (tt,  $J = 4.1$  and  $12\text{ Hz}$ ,  $\text{CH(OH)}$ , 1H), 3.73 (s,  $\text{C(=O)OCH}_3$ , 3H), 3.91 (m,  $\text{CH}_2\text{CH(OH)CH}_2$ , 1H), 4.40 (q,  $J = 6.8\text{ Hz}$ ,  $\text{C(=O)CH(CH}_3\text{)O}$ , 1H).

#### 2.6. NMRP of St initiated with **10**

St (1.0 mL, 8.7 mmol) and **10** (10 mM) were put in a glass tube, and the tube was degassed by three freeze–pump–thaw cycles with a high vacuum system and sealed off. After the tube was heated at 70–120 °C for a given time, the mixture was diluted with toluene (5 mL) and the resultant toluene

solution was poured into a large amount of MeOH. The resultant powder was collected by filtration and dried at 50 °C in a vacuum oven. For analyses, all poly(St)s obtained were once purified by reprecipitation with toluene/MeOH.

#### 2.7. Kinetic ESR study of the NO–C bond homolysis

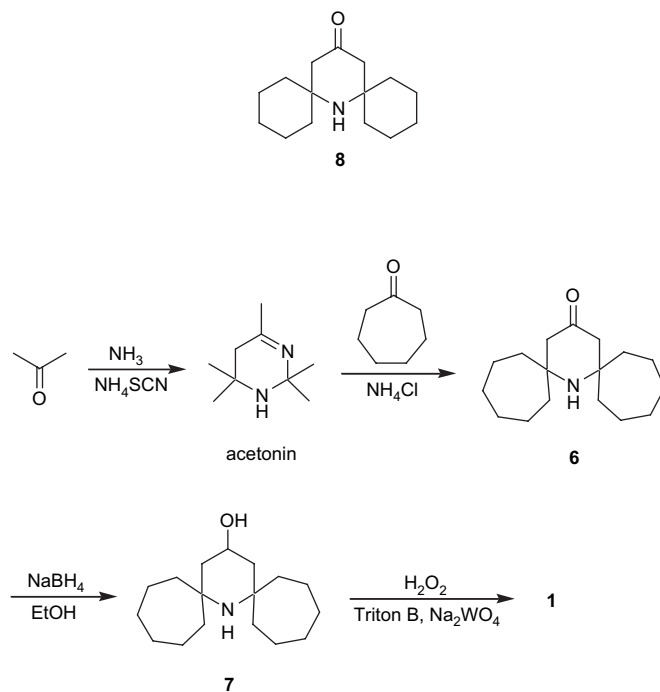
A solution of alkoxyamine ( $10\text{ mmol L}^{-1}$ ) in *tert*-butylbenzene (0.50 mL) was put in an ESR tube, and the tube was set in the cavity and heated to a constant temperature. The relative concentrations of nitroxide were determined by the double integration of the ESR signals. After the measurements were finished, the ESR tube was immediately cooled to room temperature, and the radical concentrations were determined using a calibration curve drawn using the known concentration of TEMPO solutions. ESR measurements were performed with a Bruker ESP 300 spectrometer.

### 3. Results and discussion

#### 3.1. Synthesis of nitroxide **1**

Nitroxide **1** was prepared according to Scheme 2. The reaction of acetoin with a large excess of cycloheptanone in the presence of  $\text{NH}_4\text{Cl}$  gave many byproducts.

Separation of **6** by column chromatography was difficult but **6** was isolated in 1.9% yield after repeated experiments. The result that while the reaction of acetoin with cyclohexanone gave **8** in 24% yield [17], the reaction with cycloheptanone yielded **6** in only 1.9% yield suggested that there was serious steric inhibition in the reaction. The reduction of **6** with  $\text{NaBH}_4$  gave **7** in 88% yield and the subsequent  $\text{Na}_2\text{WO}_4$ -catalyzed oxidation of **7** with  $\text{H}_2\text{O}_2$  gave **1** in 96% yield as light red needles.



Scheme 2.

### 3.2. Synthesis of alkoxyamine **9**

Alkoxyamine **9** was prepared by the reaction of DBDPX with ethylbenzene in the presence of **1**. DBDPX decomposes at room temperature in hydrocarbon solvents at a moderate rate to give *tert*-butoxyl radicals with an evolution of CO<sub>2</sub> [21]. A variety of alkoxyamines were obtained by the reaction of ethylbenzene with DBDPX in the presence of nitroxides [16,17,19,22,23]. Alkoxyamine **9** was obtained as viscous oil containing small amounts of impurities. Although the oil was subjected to preparative recycling HPLC to remove the impurities, the resulting oil was shown to contain a small amount of **1** by ESR. This ESR result suggested that the NO–C bond homolysis took place even at room temperature. The increasing amount of **1** generated by the NO–C bond homolysis of **9** in benzene at 35 °C was measured by ESR as a function of time using the method reported by Bon et al. [24]. The results are depicted in Fig. 1, and the first-order plot afforded  $1.7 \times 10^{-6} \text{ s}^{-1}$  as  $k_{\text{act}}$ . Because the **9** used for the kinetic ESR measurements contained a small amount of impurities,  $k_{\text{act}}$  will be slightly larger than  $1.7 \times 10^{-6} \text{ s}^{-1}$ .

### 3.3. Synthesis of alkoxyamine **10** and NO–C bond homolysis

Since the above results strongly suggested that isolation of pure **9** was difficult, we decided to prepare another alkoxyamine having a stronger NO–C bond. Based on the previous reports [15,25] we prepared **10** using the atom transfer method shown in Scheme 3 [26], and pure **10** was obtained as a viscous oil in 48% yield.

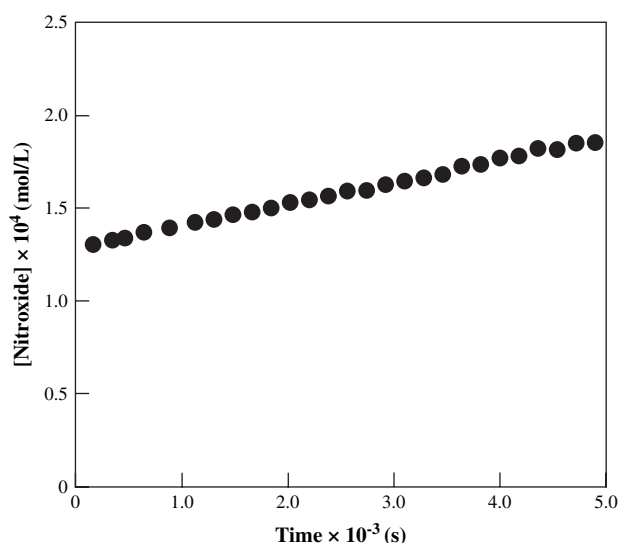
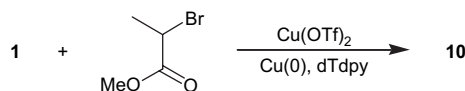


Fig. 1. Pseudo first-order plots for the NO–C bond homolysis of **9** in benzene at 35 °C. [**9**] = 10 mmol L<sup>-1</sup>.



Scheme 3.

The kinetic ESR study on the NO–C bond homolysis of **10** was performed at 60–100 °C using *tert*-butylbenzene as the solvent. In Fig. 2 the first-order plots for the homolytic reaction are shown, and  $k_{\text{act}}$ s were determined to be  $3.4 \times 10^{-6}$  (60),  $1.6 \times 10^{-5}$  (70),  $5.3 \times 10^{-5}$  (80),  $1.7 \times 10^{-4}$  (90), and  $5.2 \times 10^{-4} \text{ s}^{-1}$  (100 °C). In Fig. 3  $\ln k_{\text{act}}$ s are plotted against  $1/T$ , and the frequency factor  $A_{\text{act}}$  and the activation energy  $E_{\text{act}}$  for the NO–C bond homolysis were determined to be  $1.4 \times 10^{15} \text{ s}^{-1}$  and  $124.5 \text{ kJ mol}^{-1}$ , respectively.

In Table 1 the  $A_{\text{act}}$  and  $E_{\text{act}}$  are compared with those of some typical alkoxyamines **11**–**15**. Since the alkoxyacetyl-ethyl-releasing alkoxyamines give considerably higher  $E_{\text{act}}$ s

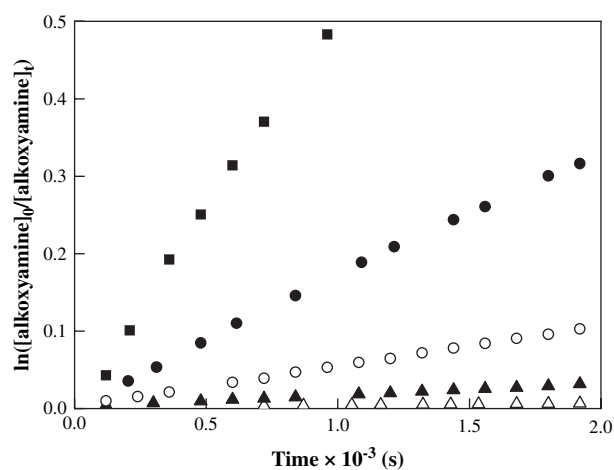


Fig. 2. First-order plots for the NO–C bond homolysis of **10** in benzene at 60–100 °C. [**10**] = 10 mmol L<sup>-1</sup>, 60 (△), 70 (▲), 80 (○), 90 (●), 100 °C (■).

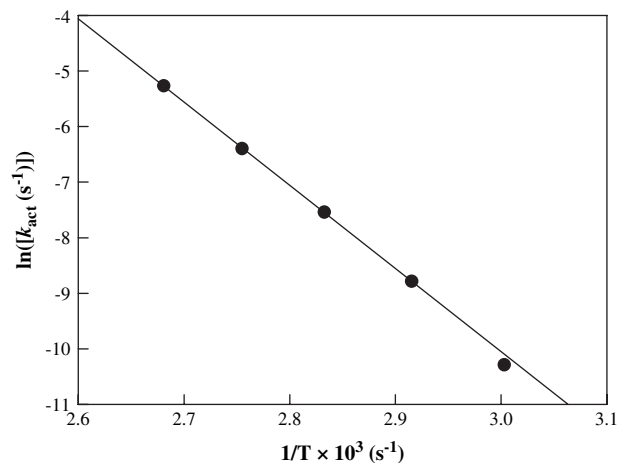


Fig. 3. Arrhenius plots of  $\ln k_{\text{act}}$  versus  $1/T$  for the NO–C bond homolysis of **10**.

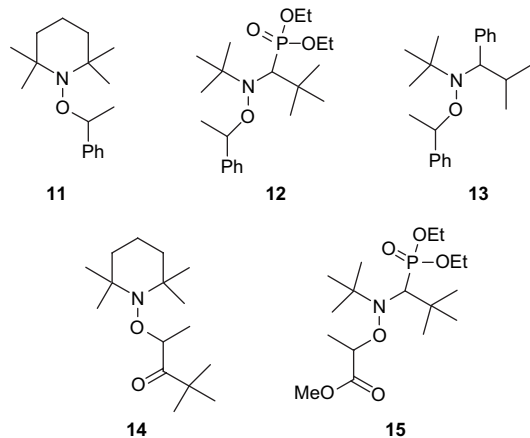
Table 1

Comparison of  $A_{\text{act}}$  and  $E_{\text{act}}$  of **10** with those of alkoxyamines **11**–**15**

Alkoxyamine	$A_{\text{act}}$ (s <sup>-1</sup> )	$E_{\text{act}}$ (kJ mol <sup>-1</sup> )	Ref.
<b>11</b>	$2.5 \times 10^{14}$	133.0	[25]
<b>12</b>	$1.9 \times 10^{14}$	124.5	[25]
<b>13</b>	$5.6 \times 10^{14}$	129.6	[25]
<b>14</b>	$1.0 \times 10^{14}$	139.0	[25]
<b>15</b>	$3.1 \times 10^{14a}$	129.7 <sup>a</sup>	[25]
<b>10</b>	$1.4 \times 10^{15}$	124.5	This work

<sup>a</sup> An average value of two isomers.

than the corresponding phenylethyl-releasing alkoxyamines [25,27], it is worth noting that **10** gives the lowest  $E_{\text{act}}$  in **10–15**. In addition, we approximated  $E_a$  for the NO–C bond homolysis of **9** to be ca 118 kJ mol<sup>-1</sup> from that of **10** using the predictive scale proposed by Marque et al. [27].



### 3.4. NMRP of St initiated with **10**

Bulk polymerization of St initiated with **10** was carried out in a degassed sealed glass tube at 70, 90, and 120 °C. Fig. 4 shows the first-order plots for the polymerization of St at 70 °C for  $[10] = 10$  and 30 mmol L<sup>-1</sup>. In both cases good linear relationships are found, demonstrating that the propagating chain numbers are constant during the polymerization.

The basic features for the NMRP were described by Fischer [8] and Fukuda et al. [9,10]. For the systems with conventional initiation a power–law analysis predicts that the monomer conversion is described by Eq. (1),

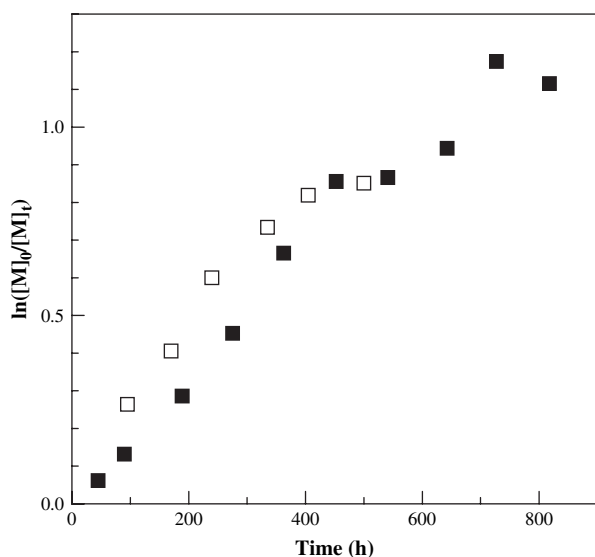


Fig. 4.  $\ln([M]_0/[M]_t)$  versus time plots for the polymerization of St initiated with **10** at 70 °C. St 1.0 mL (8.7 mmol),  $[10] = 10$  (■) and 30 mmol L<sup>-1</sup> (□).

$$\ln([M]_0/[M]_t) = k_p(R_i/k_t)^{1/2}t \quad (1)$$

where  $k_p$  and  $k_t$  are the rate constants of propagation and termination, respectively, and  $R_i$  is the rate of the thermal or conventional initiation. According to Eq. (1),  $\ln([M]_0/[M]_t)$  is proportional to time and is independent of the alkoxyamine concentration. Because St undergoes significant thermal polymerization, the present polymerization system may be described by Eq. (1) [9], even if an initiator is not added. However, Fig. 4 demonstrates that the first-order plot for  $[10] = 30$  mmol L<sup>-1</sup> is significantly larger than that for  $[10] = 10$  mmol L<sup>-1</sup>, indicating that the present polymerization system does not obey Eq. (1). Therefore, the polymerization system is not dominated by the thermal polymerization of St.

The  $M_n$  versus conversion and PDI (polydispersity index) versus conversion plots are depicted in Fig. 5. In both concentrations of **10** the observed  $M_n$  increases linearly with conversion and agrees with the theoretical  $M_n$  ( $M_{n,\text{theor}}$ ) calculated using Eq. (2). Furthermore, the PDIs are kept below 1.25 throughout the polymerization. On the basis of the above results it is concluded that **1** can control the polymerization of St at 70 °C.

$$M_{n,\text{theor}} = ([\text{Monomer}]/[\text{Alkoxyamine}]) \cdot \text{conversion} \cdot \text{MW}_{\text{St}} \quad (2)$$

The polymerization of St at 90 °C exhibited unusual results. The first-order plots are depicted in Fig. 6, and  $M_n$  versus conversion and PDI versus conversion plots are shown in Fig. 7. The first-order plots show a linear relationship until 90 h (below 60% conversion), and  $M_n$  is linearly increased with conversion, keeping PDI below 1.28. However, after 90 h the

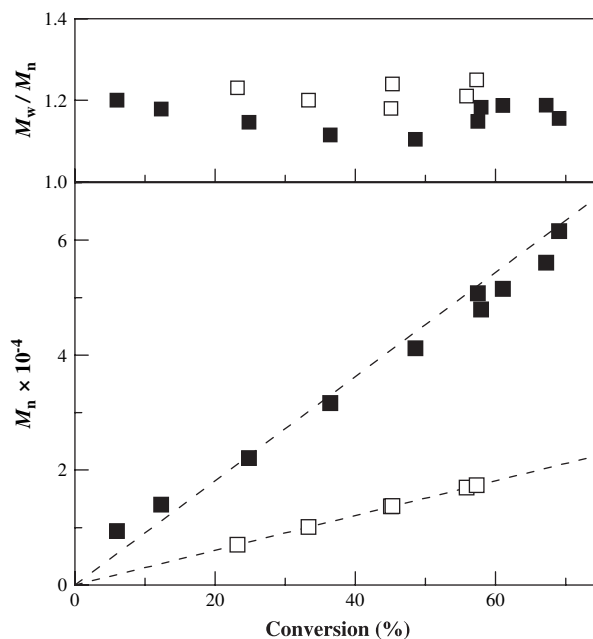


Fig. 5.  $M_n$  versus conversion and  $M_w/M_n$  versus conversion plots for the polymerization of St initiated with **10** at 70 °C. St 1.0 mL (8.7 mmol),  $[10] = 10$  (■), 30 mmol L<sup>-1</sup> (□). The calculated molecular weights are shown by dashed lines.

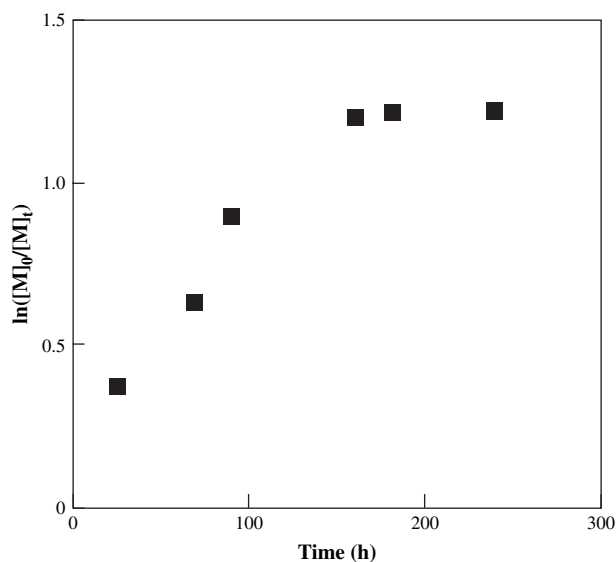


Fig. 6.  $\ln([M]_0/[M]_t)$  versus time plots for the polymerization of St initiated with **10** at 90 °C. St 1.0 mL (8.7 mmol),  $[10] = 10 \text{ mmol L}^{-1}$ .

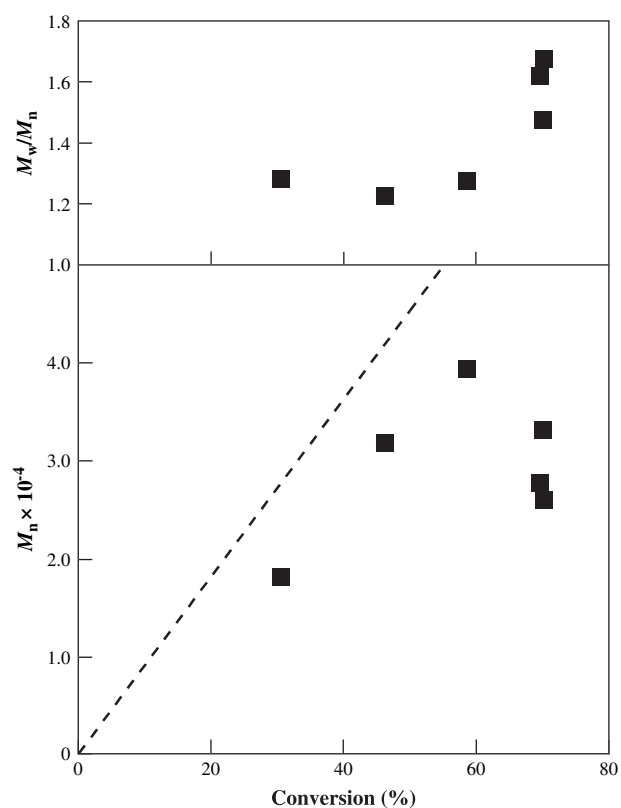


Fig. 7.  $M_n$  versus conversion and  $M_w/M_n$  versus conversion plots for the polymerization of St initiated with **10** at 90 °C. St 1.0 mL (8.7 mmol),  $[10] = 10 \text{ mmol L}^{-1}$ . The calculated molecular weights are shown by a dashed line.

polymerization rate was slow down and almost completely stopped at 160 h. During the period the  $M_n$  was decreased and the PDI was drastically increased.

To discuss the unusual polymerization behavior at 90 °C in more detail the concentration of **10** was followed as a function of time with ESR. The results are shown in Fig. 8. In the

well-controlled NMRP systems, the nitroxide concentrations are kept almost constant except for the initial stage of the polymerization [12,13,17,28,29]. However, Fig. 8 shows that the nitroxide concentration increases with time and reaches  $0.70 \text{ mmol L}^{-1}$  at 160 h. The concentration of **1** corresponds to 7% of the alkoxyamine used. The observed gradual increase in the nitroxide concentration strongly suggests that the irreversible termination reactions between the propagating chains occur to a great extent. When the nitroxide concentration reaches  $\sim 0.70 \text{ mmol L}^{-1}$ , the polymerization almost completely stops due to the too high nitroxide concentration.

In order to clarify the reason why  $M_n$  drops after 90 h (above 60% conversion), the SEC traces of the resultant poly(St)s were measured. As shown in Fig. 9, the SEC traces of 24 and 90 h were unimodal, and the PDIs were 1.15–1.28. In

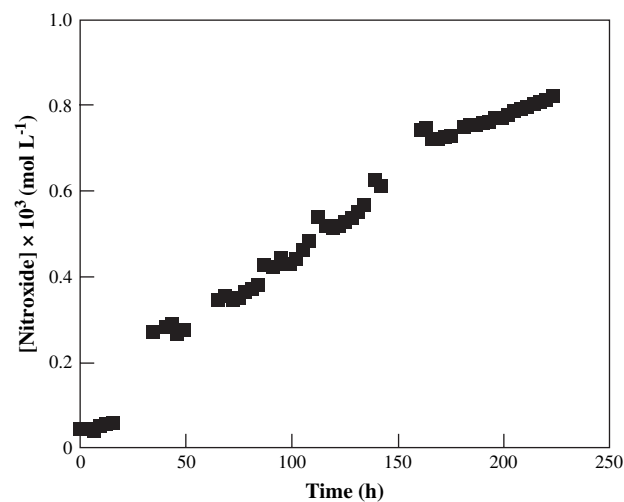


Fig. 8. Plots of the nitroxide concentration as a function of time for the polymerization of St initiated with **10** at 90 °C. St 1.0 mL (8.7 mmol),  $[10] = 10 \text{ mmol L}^{-1}$ .

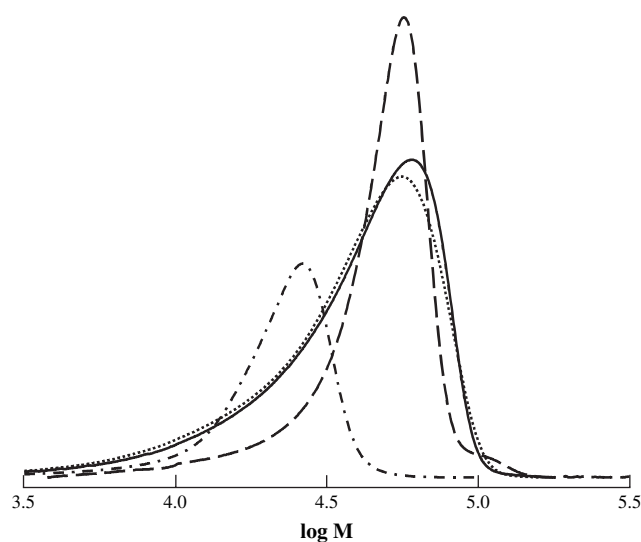


Fig. 9. SEC traces of poly(St)s obtain in the polymerization of St at 90 °C. 24 h (— · —), 91 h (— —), 161 h (····), 240 h (—).

contrast, those at 160 and 240 h are not unimodal: a broad shoulder appears in the low molecular weight region. Furthermore, no or negligible shift to a high molecular weight region is observed. The shoulder is probably due to the polymer produced by thermal polymerization of St, strongly suggesting that the thermal polymerization of St was dominated after 90 h.

The NMRP of St at 120 °C showed a quite poor control from the initial stage of the polymerization. The  $M_n$  did not show a linear relationship against conversion, and the PDI was increased with conversion and reached 1.7 at 75% conversion. Therefore, the irreversible termination reactions between the propagating chains must take place more frequently than at 90 °C.

It should be noted that since the one-end structure of the dormant species in the polymerization of St mediated by **1** is similar to that of **9**, the NO–C bond is very weak. The poor control of the polymerization of St mediated by **1** at high temperatures can be accounted for in terms of both the very fast NO–C bond homolysis of the dormant species and the slow coupling reaction between propagating chain and **1** ascribed to the steric crowding around the nitroxide moiety. It is likely that **1** suggests the upper limit in the bulkiness around the nitroxide moiety to maintain the livingness in the polymerization of St mediated with spiro ring-carrying piperidinylnitroxyl radicals [30].

#### 4. Conclusions

In this report we described the synthesis of nitroxide **1** and alkoxyamines **9** and **10** and polymerization of St mediated with **1**. We showed that alkoxyamine **9** has a very weak NO–C bond and decomposes to **1** and phenylethyl radical at room temperature. On the other hand, **10** showed a somewhat stronger NO–C bond, and  $A_{act}$  and  $E_{act}$  for the NO–C bond homolysis were determined to be  $1.4 \times 10^{15} \text{ s}^{-1}$  and  $124.5 \text{ kJ mol}^{-1}$ , respectively. The NMRPs of St mediated by **1** were performed at 70, 90 and 120 °C. Although the polymerization at 70 °C proceeded in the satisfactory living fashion to give poly(St) with narrow polydispersities, those at 90 and 120 °C showed poor control of polymerization. The

poor control of the polymerization was explained in terms of the very weak NO–C bond of the dormant species.

#### References

- [1] US Patent 4581429. Eur Pat Appl 135280. Solomon DH, Rizzardo E, Cacioli P. Chem Abstr 1985;102:221335q.
- [2] Georges MK, Veregin RPN, Kazmaier PM, Hamer GK. Macromolecules 1993;26:2987.
- [3] Hawker CJ. Acc Chem Res 1997;30:373.
- [4] Hawker CJ, Bosman AW, Harth E. Chem Rev 2001;101:3661.
- [5] Matyjaszewski K, Xia J. Chem Rev 2001;101:2921.
- [6] Kamigaito M, Ando T, Sawamoto M. Chem Rev 2001;101:3689.
- [7] Moad G, Rizzardo E, Thang SH. Aust J Chem 2005;58:379.
- [8] Fischer H. J Polym Sci Part A Polym Chem 1999;37:1885.
- [9] Fukuda T, Goto A, Ohno K. Macromol Rapid Commun 2000;21:151.
- [10] Goto A, Fukuda T. Prog Polym Sci 2004;29:329.
- [11] Benoit D, Chaplinski V, Braslau R, Hawker CJ. J Am Chem Soc 1999;121:3904.
- [12] Benoit D, Grimaldi S, Robin S, Finet JP, Tordo P, Gnanou Y. J Am Chem Soc 2000;122:5929.
- [13] Knoop CA, Studer A. J Am Chem Soc 2003;125:16327.
- [14] Bertin D, Gigmes D, Marque SRA, Tordo P. Macromolecules 2005;38:2638.
- [15] Fischer H, Kramer A, Marque SRA, Nesvadba P. Macromolecules 2005;38:9974.
- [16] Miura Y, Mibae S, Moto H, Nakamura N, Yamada B. Polym Bull 1999;42:17.
- [17] Miura Y, Nakamura N, Taniguchi I. Macromolecules 2001;34:447.
- [18] Miura Y, Nakamura N, Taniguchi I, Ichikawa A. Polymer 2003;44:3461.
- [19] Miura Y, Ichikawa A, Taniguchi I. Polymer 2003;44:5187.
- [20] Ma Z, Huang Q, Bobbitt JM. J Org Chem 1993;58:4837.
- [21] Bartlett PD, Benzing EP, Pincock RE. J Am Chem Soc 1960;82:1762.
- [22] Miura Y, Hirota K, Moto H, Yamada B. Macromolecules 1998;31:4659.
- [23] Miura Y, Hirota K, Moto H, Yamada B. Macromolecules 1999;32:8356.
- [24] Bon SAF, Chambard G, German AL. Macromolecules 1999;32:8269.
- [25] Marque S, Mercier CL, Tordo P, Fischer H. Macromolecules 2000;33:4403.
- [26] Matyjaszewski K, Woodworth BE, Zhang X, Gaynor SG, Metzner Z. Macromolecules 1998;31:5955.
- [27] Beaudoin E, Bertin D, Gigmes D, Marque SRA, Siri D, Tordo P. Eur J Org Chem 2006;1755.
- [28] Drockenmuller E, Catala JM. Macromolecules 2002;35:2461.
- [29] Fukuda T, Terauchi T, Goto A, Ohno K, Tsujii Y, Miyamoto T, et al. Macromolecules 1996;29:6393.
- [30] Siegenthaler KO, Studer A. Macromolecules 2006;39:1347.